*Article*

# Changes in Vegetation Growth Dynamics and Relations with Climate over China's Landmass from 1982 to 2011

**Guang Xu [1,2], Huifang Zhang [1,2],\*, Baozhang Chen [1],\*, Hairong Zhang [3], John L. Innes [4], Guangyu Wang [4], Jianwu Yan [1,2], Yonghong Zheng [5], Zaichun Zhu [6] and Ranga B. Myneni [6]**

[1] State Key Laboratory of Resources and Environmental Information System, Institute of Geographic Sciences and Natural Resources Research, Chinese Academy of Sciences, 11A, Datun Road, Beijing 100049, China; E-Mails: xug.12b@igsnrr.ac.cn (G.X.); yanjw2001@163.com (J.Y.)

[2] University of Chinese Academy of Sciences, Beijing 100049, China

[3] School of Environment Science and Spatial Informatics, China University of Mining and Technology, Xuzhou 221116, China; E-Mail: hairong-zhang@cumt.edu.cn

[4] Department of Forest Resource Management, University of British Columbia, 2424 Main Mall, Vancouver, BC V6T 1Z4, Canada; E-Mails: john.innes@ubc.ca (J.L.I.); guangyu.wang@ubc.ca (G.W.)

[5] School of Resource and Environmental Science, Wuhan University, 129 Luoyu Road, Wuhan 430079, China; E-Mail: zhengyh@whu.edu.cn

[6] Department of Earth and Environment, Boston University, 675 Commonwealth Avenue, Boston, MA 02215, USA; E-Mails: zhu.zaichun@gmail.com (Z.Z.), ranga.myneni@gmail.com (R.B.M.)

\* Authors to whom correspondence should be addressed; E-Mails: baozhang.chen@igsnrr.ac.cn (B.C.); zhf1268@gmail.com (H.Z.); Tel./Fax: +86-10-6488-9574.

**Abstract:** Understanding how the dynamics of vegetation growth respond to climate change at different temporal and spatial scales is critical to projecting future ecosystem dynamics and the adaptation of ecosystems to global change. In this study, we investigated vegetated growth dynamics (annual productivity, seasonality and the minimum amount of vegetated cover) in China and their relations with climatic factors during 1982–2011, using the updated Global Inventory Modeling and Mapping Studies (GIMMS) third generation global satellite Advanced Very High Resolution Radiometer (AVHRR) Normalized Difference Vegetation Index (NDVI) dataset and climate data acquired from the National

Centers for Environmental Prediction (NCEP). Major findings are as follows: (1) annual mean NDVI over China significantly increased by about 0.0006 per year from 1982 to 2011; (2) of the vegetated area in China, over 33% experienced a significant positive trend in vegetation growth, mostly located in central and southern China; about 21% experienced a significant positive trend in growth seasonality, most of which occurred in northern China (>35 °N); (3) changes in vegetation growth dynamics were significantly correlated with air temperature and precipitation ($p < 0.001$) at a region scale; (4) at the country scale, changes in NDVI was significantly and positively correlated with annual air temperature ($r = 0.52$, $p < 0.01$) and not associated with annual precipitation ($p > 0.1$); (5) of the vegetated area, about 24% showed significant correlations between annual mean NDVI and air temperature (93% positive and remainder negative), and 12% showed significant correlations of annual mean NDVI with annual precipitation (65% positive and 35% negative). The spatiotemporal variations in vegetation growth dynamics were controlled primarily by temperature and secondly by precipitation. Vegetation growth was also affected by human activities; and (6) monthly NDVI was significantly correlated with the preceding month's temperature and precipitation in western, central and northern China. The effects of a climate lag of more than two months in southern China may be caused mainly by the abundance of precipitation. These findings suggest that continuing efforts to monitor vegetation changes (*in situ* and satellite observations) over time and at broad scales are greatly needed, and are critical for the management of ecosystems and adapting to global climatic changes. It is likewise difficult to predict well future vegetation growth without linking these observations to mechanistic terrestrial ecosystem processes models that integrate all the satellite and *in situ* observations.

**Keywords:** vegetation growth dynamics; trends in NDVI; turning point; NDVI-climate relations; China

## 1. Introduction

As part of the biosphere, vegetation plays an important role in regulating the global carbon cycle [1–4]. Vegetation helps maintain climatic stability in many ways, including photosynthesis, evapotranspiration, modifying surface albedo and roughness [5,6]. There has been increasing realization of the importance of vegetation and its sensitivity to climate change [7–10]. Variations in vegetation and the relationship and interaction of vegetation with climate have become important issues in global change research [11–17]. Field surveys and remote sensing technology are commonly and widely used approaches to monitoring changes in vegetation dynamics. Field surveys can generate accurate information related to vegetation dynamics, but they are time-consuming and spatially limited [18,19]. Remote sensing technology is becoming more widely used because it is very efficient and provides high spatial and temporal resolution [20]. Jordan [21] first proposed a Simple Ratio (SR) index to describe the status of vegetation. However, in areas of high vegetation cover, measurements of this index will increase without limit. Tucker [22] proposed a normalized difference vegetation index (NDVI) that varies

between −1 and 1. The NDVI exploits the contrast in reflectance between the infrared and red portions of the electromagnetic spectrum and is well correlated to leaf area index (LAI), chlorophyll abundance, absorption of photosynthetically active radiation (fPAR) and gross primary production (GPP) quantity [7,23–25].

Many researchers have conducted studies on NDVI trends of different ecosystems and their relationships to climate change at various scales, such as the global scale [4,25–30], high northern latitudes [10,31], North America [7,17], the Hindu Kush-Himalayan region [32], the African continent [33,34] and the northern Eurasian continent [16]. China, with its varied climates, diverse ecosystems, rapid urbanization and significant land-use/land-cover change, has attracted the attention of numerous researchers. Previous studies have found that growing season vegetation cover in China increased significantly over the last three decades [10,15,35–40]. Nevertheless, several recent studies show a prominent slowdown in the positive trend of growing season NDVI during the 1980s and 1990s, which occurred in China by the mid-1990s [13,16,41]. Regarding the different trends in each season, Peng *et al.* [35] and Piao *et al.* [38] have found that NDVI in April and May (AM) has increased the most. However, detailed analysis of the monthly NDVI allows deeper understanding of interannual variation. Previous studies have also discussed vegetation dynamics at different altitudes [14,37,41] and in different ecosystems [35,37,41,42]. Different vegetative regions should also be taken into consideration as the effects of local climate may also cause differences in NDVI trends. However, while most researchers use seasonal mean NDVI data, a number of other annual NDVI indices exist (such as annual minimum NDVI and annual standard deviation) that capture other aspects of vegetation dynamics. These indices use knowledge of land cover, minimum apparent cover and seasonal variation of photosynthetic activity [43,44]. More work is needed to combine these indices, so that researchers can detect trends in vegetation dynamics using the long time series of the NDVI dataset [45].

Concerning the relationship between vegetation and climate, it has been found that temperature has a significant positive influence on vegetation growth in China [46]. Piao *et al.* [37] found a three-month lag period between the maximum trend in temperature (February) and resulting NDVI (April or May) in China. Kaspersen *et al.* [33] also find a one month lag between growing season NDVI and rainfall. Considering the delayed effects of climatic factors on NDVI values [47,48], the relationship between monthly NDVI and the lag effect of temperature and precipitation and its spatial pattern needs deeper exploration

Previous findings and the current research mentioned above led to our research questions: How has the level of greenness observed in different months in China changed over the past three decades? What are the regional patterns of change in these vegetation dynamics (mean and minimum NDVI, and its variation) and how are they linked with vegetation regionalization? How do the effects of temperature and precipitation on vegetation dynamics differ spatially? How do the delayed effects of climate occur temporally and spatially?

In this study, we first analyzed changes in annual, growing season and monthly mean NDVI, annual apparent minimum NDVI and its annual standard deviation for each vegetated pixel and these changes at the vegetation region scale. We then explored the relationship between changes in NDVI and the climatic factors (temperature and precipitation) to gain further insight into the contributions of climate to changes in vegetation. A piecewise regression model was applied to the trend and turning point (TP) analyses over the last three decades. As only a small proportion of the land surface area has had

obvious disturbances over the last 30 years [49], errors from land use change are negligible [50] and were not be analyzed in detail.
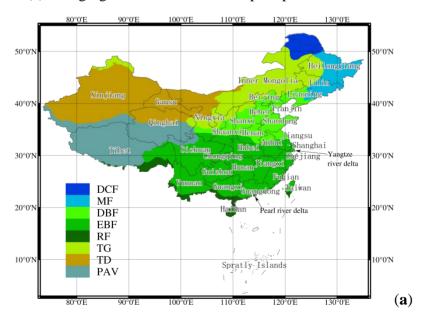
## 2. Datasets and Methods

### 2.1. Datasets

We used the Global Inventory Modeling and Mapping Studies (GIMMS) third-generation NDVI dataset derived from Advanced Very High Resolution Radiometer (AVHRR) sensors (NDVI3g) at 1/12 degree (0.0825 degree) spatial resolution and a 15-day interval, spanning July 1981 to December 2011. This dataset was developed under the framework of the GIMMS project. The GIMMS NDVI datasets have been corrected to minimize various deleterious effects, such as calibration loss, orbital drift and volcanic eruptions, and are suitable for identifying long-term trends in vegetation activity [36,39]. We generated monthly NDVI by applying the maximum value composite method from the two NDVI images of each month, to reduce noise in the NDVI data [51]. Any pixels with a 30-year averaged NDVI value less than 0.1 were considered non-vegetated areas [37,52] and were masked out.

We used air temperature at 2 m above ground level and precipitation rate, taken from NCEP Climate Forecast System Reanalysis and its version 2 (CSFV2) products [53,54], with spatial resolution 0.5 degree and 6-hour intervals. This dataset spans the period from January 1979 to December 2011. To match the resolutions and scales of meteorological data with the NDVI3g data, we averaged the meteorological data to monthly and yearly values, and resampled them to a spatial resolution of 1/12 degree using the nearest neighbor method.

**Figure 1.** (**a**) Regional vegetation map of China. [55] DCF, cold temperate deciduous-coniferous forest; MF, temperate coniferous and broadleaf mixed forest; DBF, warm temperate deciduous broadleaf forest; EBF, subtropical evergreen broadleaf forest; RF, tropical monsoon and rain forest; TG, temperate grassland; TD, temperate desert; PAV, Qinghai-Tibet Plateau alpine vegetation; (**b**) Changing trend in mean annual temperature and (**c**) changing trend in mean annual precipitation.
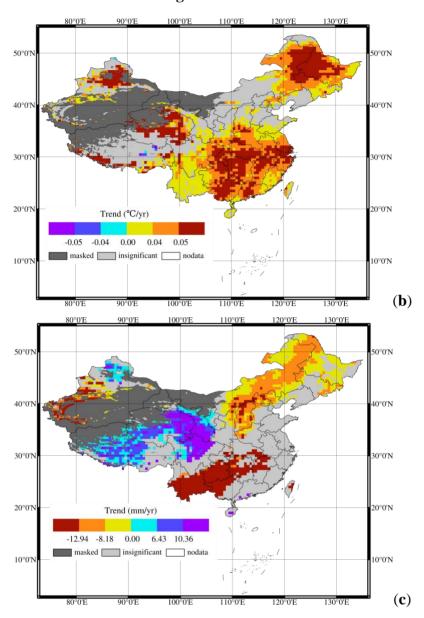


(**a**)

**Figure 1.** *Cont.*



(b)



(c)

The vegetation map of China, based on different landforms, climate, soil and human activity, produced by the Institute of Botany, Chinese Academy of Sciences [55], was used for analysis of different regions. China was separated into eight vegetation regions (Figure 1), as follows: (1) cold temperate deciduous coniferous forest (DCF); (2) temperate coniferous and broadleaf mixed forest (MF); (3) warm temperate deciduous broadleaf forest (DBF); (4) subtropical evergreen broadleaf forest (EBF), (5) tropical monsoon and rainforest (RF); (6) temperate grassland (TG); (7) temperate desert (TD) and (8) Qinghai-Tibet Plateau alpine vegetation (PAV). This regionalized map has been relatively stable over the past three decades, with less uncertainty than land-cover or land-use data

*2.2. Methods*

A linear regression model was used to detect trends in NDVI time series, and an F-test was used to check for statistical significance. Considering the potential TP in the NDVI time series, we also used a piecewise regression model [56] to see if trends in NDVI changed over the study period.

$$\mathrm{NDVI}_i = \begin{cases} b_0 + b_1 t_i + \varepsilon, t_i \le t_k \\ b_0 + b_1 t_i + b_2(t_i - t_k) + \varepsilon, t_i > t_k \end{cases} \tag{1}$$

where *NDVI$_i$* is the NDVI time series, $t_i$ is time, and $t_k$ is the TP; when $t_i$ is before $t_k$, the slope of *NDVI$_i$* is $b_1$. After $t_k$, the slope of *NDVI$_i$* is $b_1 + b_2$. In addition, $k$ is limited to between 4 and n–3, to avoid using a segment that is too short before or after the TP. The model parameters are estimated using the maximum likelihood method. This model has been widely applied in many previous studies [16,17,41,57–60]. We fitted the models to the NDVI time-series data using the maximum likelihood (least-squares error) method, and evaluated to see if the TPs were significant using the Akaike Information Criterion (AIC) [61]. The AIC value of a regression model (either normal regression model or piecewise regression model) is defined as

$$\mathrm{AIC} = \mathrm{nlog}\left(\frac{\mathrm{RSS}}{\mathrm{n}}\right) + 2\mathrm{k} + \frac{2\mathrm{k}(\mathrm{k}+1)}{\mathrm{n}-\mathrm{k}-1} \tag{2}$$

where *RSS* is the residual sum of squares, *n* is the sample size, and *k* is the number of parameters in the regression model. If the difference between the AIC values of the two models is greater than 2, the model with the lower AIC value is considered more effective, *i.e.*, if AIC value of the piecewise regression model is less than that of the normal regression model by −2, the TP is considered significant [62]. Using this method, we determined whether the NDVI time series should be fitted using the linear regression or piecewise regression model. Furthermore, the trend of the TP will change significantly if the null hypothesis of $b_2 = 0$ is rejected, as occurs with the difference between the trend before and after the TP.

In addition, we applied Spearman partial correlation analysis to the monthly and annual NDVI time series data and climate factors (temperature and precipitation) to provide robust insights into their correlations, taking into account the nonlinear relationship and interaction between dynamic vegetation indices and climatic variables (temperature and precipitation). A lag time is defined as the number of months after which the NDVI shows the highest significant positive correlation coefficient with previous temperature or precipitation. The lag time is assumed to be limited to less than 6 months, based on the Ren *et al.* [63] finding that the effect of climate factors can persist into the next season.

One-way analysis of variance was used to test whether there is an overall difference between trends in different vegetation regions. The Games-Howell post hoc [64] analysis was used to check if vegetation regions were significantly different from each other.
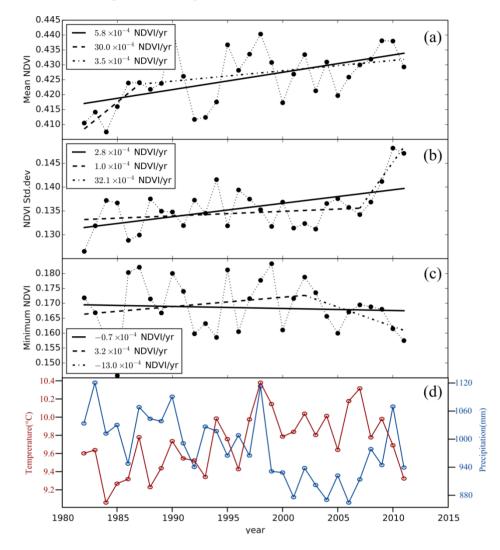
## 3. Results and Discussion

### *3.1. NDVI Trends*

#### 3.1.1. Trends at Country Scale

To investigate the overall trend of NDVI in China, regionally averaged mean, standard deviation and minimum of NDVI for each year were calculated and their linear trends were analyzed (Figure 2).

**Figure 2.** Trends of (**a**) annual mean; (**b**) standard deviation and (**c**) minimum of NDVI and (**d**) air temperature/precipitation, from 1982 to 2011. Solid line is the linear regressive line. The dashed line is piecewise regressive line.



The mean NDVI of China increased significantly from 1982 to 2011 ($5.8 \times 10^{-4}$ NDVI·yr$^{-1}$ or 0.14% yr$^{-1}$; $p = 0.002$), which was close to the growing season NDVI trend (0.0007 NDVI·yr$^{-1}$) in China from 1982 to 2010 [35] and slightly lower than the NDVI trend ($6.22 \times 10^{-4}$ NDVI·yr$^{-1}$) in Asia-Australia region [50]. The TP was in 1987. Before that TP, annual mean NDVI increased at a high rate (0.003 NDVI·yr$^{-1}$ or 0.73% yr$^{-1}$; $p = 0.247$). Afterward, the rate of increase fell to 0.00035 NDVI·yr$^{-1}$ or 0.08% yr$^{-1}$ ($p = 0.176$), which can be attributed to urbanization in China during the 1990s [58]. The AIC values of the linear regression and piecewise regression models were 266.87 and 266.10, respectively. The difference (0.77) is less than 2, indicating that no significant TP existed at national scale and vegetation cover in the country has continued to increase since 1982, consistent with the findings of Peng *et al.* [35] and Sun *et al.* [58].

The standard deviation of NDVI in China also increased significantly from 1982 to 2011 ($2.8 \times 10^{-4}$ NDVI·yr$^{-1}$ or 0.21% yr$^{-1}$; $p = 0.003$). The AIC test shows that there is a significant presence of a TP in the year 2007. The standard deviation of NDVI increased slightly ($1.0 \times 10^{-4}$ NDVI·yr$^{-1}$ or 0.08% yr$^{-1}$; $p = 0.48$) before 2007 and increased rapidly after that ($32.1 \times 10^{-4}$ NDVI·yr$^{-1}$ or

2.37% yr$^{-1}$; $p$ = 0.059), indicating that seasonal changes of vegetation have increased significantly, especially after 2007. In contrast, the annual minimum of NDVI decreased from 1982–2011 (0.7 $\times$ 10$^{-4}$ NDVI·yr$^{-1}$ or ~0.04% yr$^{-1}$; $p$ = 0.73). The AIC test for this value indicated that no significant TP existed. We also compared the trends using annual mean NDVI *vs.* growing season mean values and found that the identified trends and changes in trends are similar. The trend in annual or growing season NDVI is an average of trends in each month. To detect more detailed changing signals at finer temporal scales, we conducted the same analysis at monthly scales.

### 3.1.2. NDVI Trends in Each Month

Monthly trends of NDVI were also analyzed (Table 1). Over the past three decades, monthly mean NDVI in China increased in most growing months. The overall trends in NDVI were statistically significant for April, May, July, August and September, peaking in April and May, suggesting NDVI increased the most in spring [35,37]. Significant TPs of monthly mean NDVI were detected for June 1984, July 1988 and August 2007. The TPs vary because monthly NDVI values are independent of each other and can have different trends. The monthly mean overall NDVI of June and July increased rapidly before the TP, that of June decreased after the TP, and that of July stabilized after the TP. By contrast, annual mean NDVI in August stabilized from 1982 through 2007 (the TP year), and increased at a high rate (0.011 NDVI yr$^{-1}$ or 1.71% yr$^{-1}$) after the TP.

**Table 1.** Trends and TPs of NDVI for entire study area, in each month from 1982 to 2011.

| Month | Mean NDVI | Overall Trend ($\times 10^{-5}$ NDVI·yr$^{-1}$) | TP | Trend Before TP ($\times 10^{-5}$ NDVI·yr$^{-1}$) | Trend After TP ($\times 10^{-5}$ NDVI·yr$^{-1}$) | AIC |
|---|---|---|---|---|---|---|
| 1 | 0.27 | −24.0 | 1999 | 65 | −172 | −0.95 |
| 2 | 0.26 | 14.4 | 1987 | 531 | −35 | 0.19 |
| 3 | 0.28 | 40.0 | 2001 | 119 | −162 | 0.25 |
| 4 | 0.34 | 166.9 * | 1998 | 246 | 61 | 1.87 |
| 5 | 0.50 | 134.7 * | 1990 | 400 | 71 * | −1.36 |
| 6 | 0.56 | 15.1 | 1984 | 2201 | −27 | −8.59 * |
| 7 | 0.63 | 53.3 * | 1988 | 399 | 6 | −4.08 * |
| 8 | 0.64 | 62.3 * | 2007 | −3 | 1088 | −13.1 * |
| 9 | 0.59 | 105.6 * | 2003 | 82 | 203 | 2.02 |
| 10 | 0.43 | 85.8 | 2000 | 28 | 204 | 2.21 |
| 11 | 0.33 | 61.8 | 2009 | 93 | −1566 | −1.24 |
| 12 | 0.29 | −16.4 | 2008 | 0.8 | −466 | 2.01 |

* indicates a significant TP in terms of AIC.
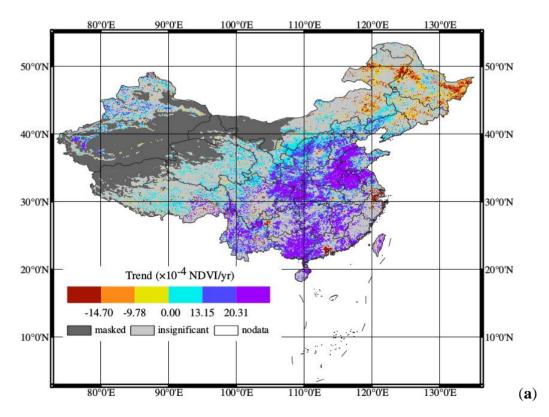
### 3.1.3. Spatial Pattern of NDVI Trends

The three indicators, the annual mean, minimum and standard deviation of NDVI, were calculated for each pixel to represent vegetation productivity, minimum apparent coverage and seasonality, respectively, and their trends from 1982 to 2011 are shown (Figure 3). Dark gray represents non-vegetated area, and was identified by a 30-year average NDVI less than 0.1. This sparsely
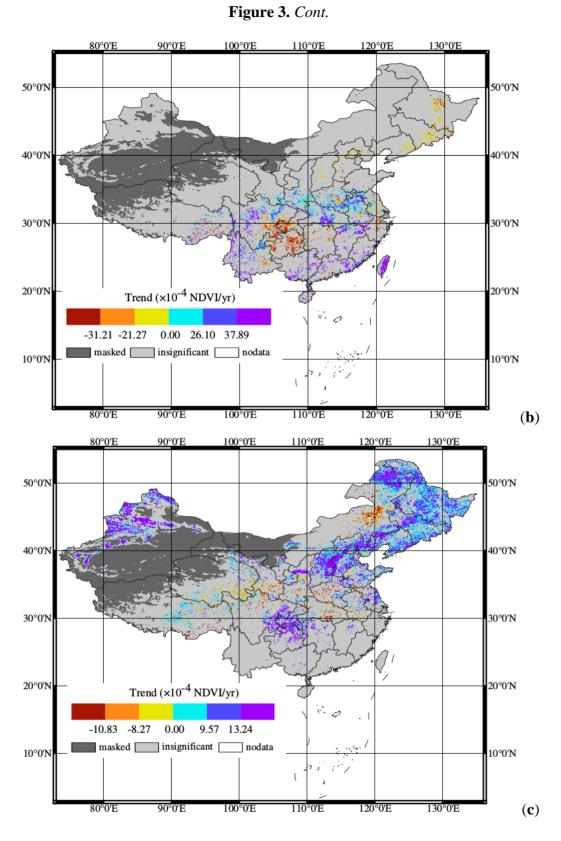
vegetated area constitutes 22.5% of the study area, and is mainly located in southern Xinjiang (desert) and northern Tibet (ice/snow cover).

From 1982 to 2011, annual mean NDVI increased significantly over 33% of the vegetated area (Figure 3a), most of these pixels were observed in central and southern China, mainly located in the following three regions: subtropical evergreen broadleaf forest, warm temperate deciduous broadleaf forest and tropical monsoon and rain forest. The annual NDVI declined sharply in the Yangtze and Pearl River deltas, because of rapid urban expansion over the past 30 years [37,65]. Also, the regions where annual mean NDVI decreased significantly (≈8% of vegetated area in the country) were mainly observed in northeastern China; this decrease is likely to be related to agricultural reclamation [65], consistent with the findings of Mao *et al.* [66] NDVI tended to decrease significantly in forest- dominated regions of the northeast China.

A small proportion (≈9%) of the vegetated area had a significant trend in minimal vegetation cover (Figure 3b; about 60% trending positive and 40% negative); these pixels were mostly located in subtropical evergreen broadleaf forest. There were areas with a significant positive trend in minimum annual NDVI (at a rate greater than 0.0035 $yr^{-1}$) in Jiangxi, Hunan and Hubei provinces There was a negative trend area in southwestern China, where extreme drought occurred in the late 2000s [67].

**Figure 3.** Trends of (**a**) annual mean; (**b**) annual minimum and (**c**) annual standard deviation of NDVI in study area. White pixels represent no data, light gray pixels indicate an insignificant trend, and dark gray pixels are masked with threshold of 30-year mean NDVI < 0.1.



(**a**)

**Figure 3.** *Cont.*
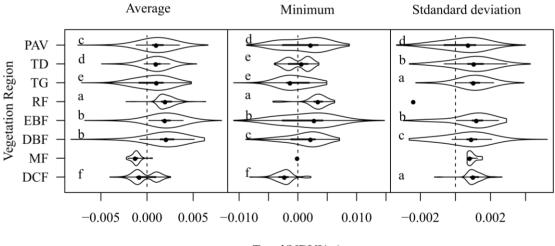


(**b**)



(**c**)

About 24% of China's vegetated land showed a significant trend in vegetation seasonality (indicated by the annual standard deviation of NDVI, Figure 3c). In terms of seasonality, the areas with positive and negative trends accounted for about 21% and 3% of the vegetated area, respectively; northern China (north of 35 °N) had positive trends; most regions (cold temperate deciduous coniferous

forest, temperate coniferous and broadleaf mixed forest, and warm temperate deciduous broadleaf forest) had increasing trends.

In general, the growth of vegetation and its seasonal changes in the study area increased from 1982–2011, while areas with minimum apparent vegetation cover changed only marginally. Violin plots [68], a combination of box plot and histogram were used to illustrate the different trends over different vegetation regions (Figure 4). Analysis of variance shows that the impacts of vegetation region on the trends in annual average, minimum and standard deviation of NDVI are significant ($p < 0.001$). Post hoc comparison shows that the annual mean NDVI over vegetation regions of RF, EBF and DBF had the most significant positive trends, followed by PAV and TD. Conversely, the annual mean NDVI of MF and DCF had the most significant decreasing trends. In addition, the annual minimum NDVI had the most significant positive and negative trends in RF and DCF. The trends of annual standard deviation of NDVI for all vegetation regions were significantly positive, except for RF.

**Figure 4.** Violin plots of trends of annual average/minimum/standard deviation of NDVI at each pixel in each vegetation region. The black dots indicate the mean values; the short-segments indicate the interquartile range, as in standard box plots. Overlaid on them are kernel density estimations. Grouping results of Games-Howell post hoc pairwise comparison analyses are labeled with letters on the left. Regions with an insufficient number of pixels (<100) with significant trends were excluded from post hoc tests. Vegetation regions with the same letter have insignificant differences in trends. Average trends from positive to negative are labeled in alphabetical order.



Grassland degradation in the Tibetan Plateau reported by Zhou *et al.* [69] and Cui *et al.* [70] was not evident in this study mainly because the Tibetan Plateau was sparsely vegetated and had low NDVI values (<0.3). It is most difficult for linear trends in NDVI time series with low values to reach a significance level because of potential noise. Moreover, most of the severely degraded grassland was observed in the headwater areas of the Yangtze and Yellow Rivers [70], which was a local or small scale phenomenon and beyond the capacity of AVHRR based vegetation data set (~64 km per pixel). This is also a limitation of our research.

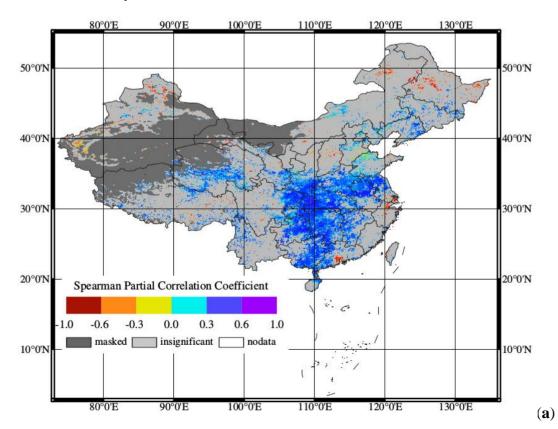## 3.2. Relationship between NDVI and Climatic Factors

### 3.2.1. Relationship with Climatic Factors at a Country Scale

The time series of annual average NDVI values from 1982 to 2011 at the country scale was significantly and positively correlated with air temperature ($r = 0.52$, $p < 0.01$), but insignificantly correlated with annual precipitation ($r = -0.05$, $p = 0.79$). Thus, the overall greening trends in the study area are likely caused by the overall rate of increase in temperature (0.019 °C per year; $p = 0.004$) in China. The statistical analysis revealed that inter-annual variation of NDVI was dominantly linked to warming, and less influenced by variations in annual precipitation.

### 3.2.2. Spatial Pattern of NDVI-Climate Relationships

The positive correlation between the overall greening trend and warming trend may vary with vegetation region. The correlation coefficients between NDVI and climate factors at each pixel are shown in Figure 5. In about 23.9% and 12.0% of the vegetated area, annual mean NDVI was correlated significantly with annual mean air temperature and precipitation, respectively, suggested that in larger areas vegetation growth was controlled by temperature in China. This is consistent with previous findings [46,66].

**Figure 5.** Map of correlation coefficients between annual mean NDVI with (**a**) annual mean air temperature and (**b**) annual total precipitation. White areas represent pixels with no data, light gray pixels represent insignificant trends, and dark gray pixels are masked with threshold of 30-year mean NDVI < 0.1.
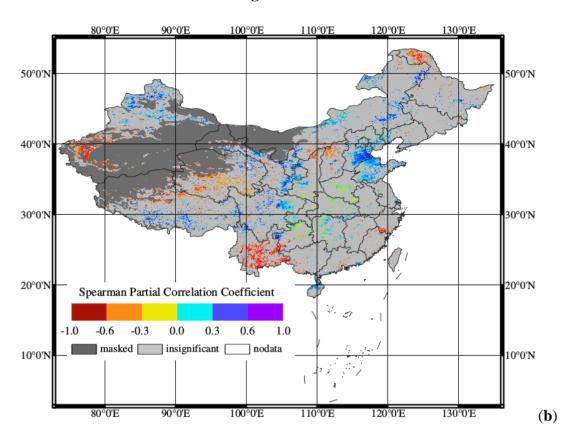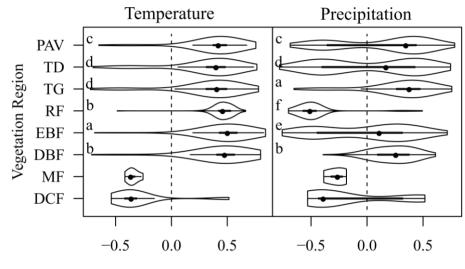


(**a**)

**Figure 5.** *Cont.*



(**b**)

Areas where NDVI was positively correlated with air temperature were dominant (92.76% of the significantly correlated area; Figure 5a). Only about 7.24% of the significant temperature-correlated area was negative, mainly in northeastern China (*i.e.*, northern Xinjiang). The significant negative correlation in the Pearl and Yangtze River delta areas is probably spurious, caused by a heat island effect and vegetation degradation, which may be the result of continued rapid urbanization. Examinations of interactions between land-use change and NDVI dynamics are beyond the scope of this study, but represent an important topic of future research.

In about 12% of the vegetated area, annual NDVI was correlated significantly with annual precipitation, with 64.3% positive and 35.7% negative. In southwestern China, the northern portion of northeastern China and western Xinjiang, the annual NDVI was significantly and negatively related to annual precipitation. In the southern Qinghai-Tibet Plateau, Hebei and Shandong provinces, and north Xinjiang, the annual NDVI was significantly and positively correlated with annual precipitation (Figure 5b). The negative correlation between NDVI and precipitation in the northern part of northeastern China was attributed to the large number of cloudy days caused by precipitation during the cold and snowy spring weather there [37,66]. The negative correlation on the Tibetan Plateau could be attributed to the increasing snow and ice cover caused by increasing precipitation [37]. The negative correlation of annual NDVI with precipitation in southwestern China may be tied to precipitation-related decreases of temperature [37], increases of cloud cover, and a reduction of incoming solar radiation.

The violin plots [68] of correlation coefficients for each vegetation region are shown in Figure 6. The impacts of vegetation regions on the correlations between NDVI and temperature and precipitation were significant ($p < 0.001$). Post hoc comparison shows that EBF had the strongest positive

correlation with temperature, followed by DBF > RF > TG > TD > PAV. The annual NDVI for MF and DCF showed significant and negative correlation with annual temperature. TG, DBF, PAV, TD and EBF had the strongest positive correlations with annual precipitation. A negative correlation with precipitation was found only for RF.

> **Figure 6.** Violin plots of correlation coefficients between annual NDVI and temperature and precipitation at each pixel in each vegetation region. Grouping results of Games-Howell post hoc pairwise comparison analysis are labeled with letters at left. Regions with an insufficient number of pixels (<100) with significant correlations are excluded from post hoc tests. Vegetation regions with the same letters have insignificant differences in correlations. Average correlations from positive to negative are labeled in alphabetical order.
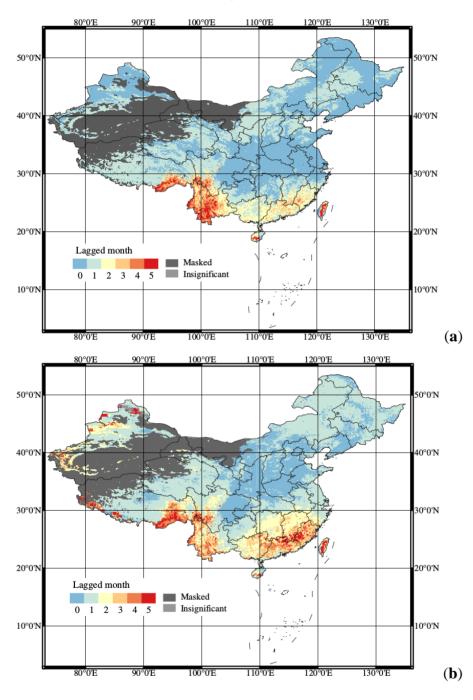


### 3.2.3. Spatial Pattern of Time Lags

The climatic factors may have delayed effects on monthly NDVI, which can vary by region. Therefore, the time lags of each pixel were calculated (Figure 7). Most unmasked pixels showed significant positive correlations between monthly NDVI and corresponding monthly temperature and precipitation, with a lag time less than 6 months (99.63% and 99.17%, respectively), of which pixels with zero and one-month lag constituted a large proportion (87.40% and 76.06%). These were mainly in western, central and northern China. Precipitation was more likely to have a lag effect (74.83%) than temperature (51.90%). Monthly NDVI was remarkably related with both temperature and precipitation after more than two months in southern and southwestern China, where the monthly averages of temperature, precipitation and NDVI were all high. The spatial patterns of precipitation time lag agree with the conclusion that the response of NDVI to precipitation is faster when soils and vegetation are drier [48]. In contrast, areas with high precipitation stayed green longer when soil moisture was high [71]. Therefore, in humid areas, precipitation had a longer time-lag effect.

**Figure 7.** Map of lagged months of (**a**) temperature and (**b**) precipitation. White area represents pixels with no data, light gray pixels represent insignificant trends, and dark gray pixels are masked with threshold of 30-year mean NDVI < 0.1.



(**a**)



(**b**)

## 4. Conclusions and Implications

The spatiotemporal variations in vegetation growth dynamics (three indicators) and their relations with climatic factors in China were investigated using the AVHRR NDVI data and NCEP air temperature and precipitation data during 1982–2011. The following conclusions were drawn:

(1) The overall annual NDVI in China showed a significant positive trend from 1982 to 2011 ($\approx$0.0006 yr$^{-1}$ or 0.14% yr$^{-1}$, $p = 0.002$).

(2) The monthly mean NDVI in June, July and August had a significant TP in1984, 1988 and 2007, respectively. The monthly mean NDVI increased rapidly in June and July prior to the TPs and decreased for June and mostly stalled in July after the TPs; while in August the annual mean NDVI stabilized prior to the TP and rapidly increased after the TP at a rate of 0.011 NDVI·yr$^{-1}$ (1.71% yr$^{-1}$).

(3) Of the vegetated area in China, about 33% showed a significant positive trend in annual mean NDVI, being mostly located in central to southern China; about 21% showed a significant positive trend in seasonality (s.d. NDVI), being most located in northern China (>35 °N); a small proportion (<9%) had a significant trend in minimum vegetation coverage, with about half positive (in Jiangxi, Hunan and Hubei provinces, mainly caused by tree plantations) and half negative (in southwestern China, mainly caused by drought in the 2000s).

(4) At the vegetation region scales, changes in vegetation growth dynamics were significantly correlated with air temperature ($p < 0.001$); at the country scale, changes in NDVI was significantly and positively correlated with annual air temperature ($r = 0.52$, $p < 0.01$) and insignificantly correlated with annual precipitation ($p > 0.1$).

(5) In about 24% of the vegetated area, annual mean NDVI was correlated significantly with air temperature (93% positive and remainder negative); and in 12% of the vegetated area, annual mean NDVI was correlated significantly with annual precipitation (65% positive and 35% negative).The spatiotemporal variations in vegetation growth dynamics were controlled primarily by temperature and secondly by precipitation. Vegetation growth was also affected by human activities, such as plantations, urbanization and agricultural practices in some regions.

(6) Monthly NDVI was significantly correlated with the preceding month's temperature and precipitation in western, central and northern China. The effects of a climate lag of more than two months in southern China may mainly be caused by the abundance of precipitation.

The results presented in this study demonstrate that annual vegetation productivity and seasonality in China vary among different vegetation regions. These different spatial patterns of gradual changes and TPs indicate complexity in vegetation growth dynamics and a nonlinear response of vegetation to global climatic changes and other drivers. The mechanisms behind the temporal and spatial dynamics of vegetation productivity in the context of accelerated global environmental change are not well understood. Divergence between the findings and those of previous researchers using different lengths of NDVI data series at different scales, suggests that continuing efforts to monitor vegetation changes (*in situ* and satellite observations) over time and at broad scales are greatly needed and critical for the management of ecosystems, biodiversity, and for diagnosing and adapting to global climatic changes. Moving forward it is difficult to understand vegetation dynamics and its interaction with global climatic change. It is likewise difficult to predict well future vegetation growth and carbon sinks, without linking these observations to mechanistic terrestrial ecosystem processes models which integrate all the satellite and *in situ* observations.

## Acknowledgments

## Author Contributions

All authors contributed extensively to the work presented in this paper. Baozhang Chen designed the research. Guang Xu and Huifang Zhang analyzed the data. Baozhang Chen, Guang Xu and Huifang Zhang interpreted the results and wrote the paper. Hairong Zhang, John L. Innes, Guangyu Wang, Jianwu Yan, Yonghong Zheng, Zaichun Zhu and Ranga B. Myneni aided with the results interpretation, discussion and editing the paper.

## Conflicts of Interest

The authors declare no conflict of interest.

## References

1. Ciais, P.; Reichstein, M.; Viovy, N.; Granier, A.; Ogée, J.; Allard, V.; Aubinet, M.; Buchmann, N.; Bernhofer, C.; Carrara, A. Europe-wide reduction in primary productivity caused by the heat and drought in 2003. *Nature* **2005**, *437*, 529–533.
2. Peylin, P.; Bousquet, P.; Le Quéré, C.; Sitch, S.; Friedlingstein, P.; McKinley, G.; Gruber, N.; Rayner, P.; Ciais, P. Multiple constraints on regional $CO_2$ flux variations over land and oceans. *Glob. Biogeochem. Cy.* **2005**, *19*, doi:10.1029/2003gb002214.
3. Schwalm, C.R.; Williams, C.A.; Schaefer, K.; Arneth, A.; Bonal, D.; Buchmann, N.; Chen, J.; Law, B.E.; Lindroth, A.; Luyssaert, S. Assimilation exceeds respiration sensitivity to drought: A fluxnet synthesis. *Glob. Chang. Biol.* **2010**, *16*, 657–670.
4. Zhao, M.; Running, S.W. Drought-induced reduction in global terrestrial net primary production from 2000 through 2009. *Science* **2010**, *329*, 940–943.
5. Anderson, R.G.; Canadell, J.G.; Randerson, J.T.; Jackson, R.B.; Hungate, B.A.; Baldocchi, D.D.; Ban-Weiss, G.A.; Bonan, G.B.; Caldeira, K.; Cao, L.; *et al.* Biophysical considerations in forestry for climate protection. *Front. Ecol. Environ.* **2011**, *9*, 174–182.
6. Jackson, R.B.; Randerson, J.T.; Canadell, J.G.; Anderson, R.G.; Avissar, R.; Baldocchi, D.D.; Bonan, G.B.; Caldeira, K.; Diffenbaugh, N.S.; Field, C.B. Protecting climate with forests. *Environ. Res. Lett.* **2008**, *3*, doi:10.1088/1748-9326/3/4/044006.
7. Goetz, S.J.; Bunn, A.G.; Fiske, G.J.; Houghton, R. Satellite-observed photosynthetic trends across boreal North America associated with climate and fire disturbance. *Proc. Natl. Acad. Sci. USA* **2005**, *102*, 13521–13525.

8.  Myneni, R.B.; Keeling, C.; Tucker, C.; Asrar, G.; Nemani, R. Increased plant growth in the northern high latitudes from 1981 to 1991. *Nature* **1997**, *386*, 698–702.

9.  Piao, S.; Ciais, P.; Huang, Y.; Shen, Z.; Peng, S.; Li, J.; Zhou, L.; Liu, H.; Ma, Y.; Ding, Y. The impacts of climate change on water resources and agriculture in China. *Nature* **2010**, *467*, 43–51.

10. Zhou, L.; Tucker, C.J.; Kaufmann, R.K.; Slayback, D.; Shabanov, N.V.; Myneni, R.B. Variations in northern vegetation activity inferred from satellite data of vegetation index during 1981 to 1999. *J. Geophy. Res.* **2001**, *106*, 20069–20083.

11. Hall-Beyer, M. Comparison of single-year and multiyear NDVI time series principal components in cold temperate biomes. *IEEE Trans. Geosci. Remote Sens.* **2003**, *41*, 2568–2574.

12. Kawabata, A.; Ichii, K.; Yamaguchi, Y. Global monitoring of interannual changes in vegetation activities using NDVI and its relationships to temperature and precipitation. *Int. J. Remote Sens.* **2001**, *22*, 1377–1382.

13. Park, H.S.; Sohn, B. Recent trends in changes of vegetation over east asia coupled with temperature and rainfall variations. *J. Geophy. Res.* **2010**, *115*, doi:10.1029/2009JD012752.

14. Piao, S.; Cui, M.; Chen, A.; Wang, X.; Ciais, P.; Liu, J.; Tang, Y. Altitude and temperature dependence of change in the spring vegetation green-up date from 1982 to 2006 in the Qinghai-Xizang plateau. *Agric. For. Meteorol.* **2011**, *151*, 1599–1608.

15. Piao, S.; Fang, J.; Zhou, L.; Ciais, P.; Zhu, B. Variations in satellite-derived phenology in China's temperate vegetation. *Glob. Chang. Biol.* **2006**, *12*, 672–685.

16. Piao, S.; Wang, X.; Ciais, P.; Zhu, B.; Wang, T.; Liu, J. Changes in satellite-derived vegetation growth trend in temperate and boreal Eurasia from 1982 to 2006. *Glob. Chang. Biol.* **2011**, *17*, 3228–3239.

17. Wang, X.; Piao, S.; Ciais, P.; Li, J.; Friedlingstein, P.; Koven, C.; Chen, A. Spring temperature change and its implication in the change of vegetation growth in North America from 1982 to 2006. *Proc. Natl. Acad. Sci. USA* **2011**, *108*, 1240–1245.

18. Li, X.; Jia, X.; Dong, G. Influence of desertification on vegetation pattern variations in the cold semi-arid grasslands of Qinghai-Tibet plateau, north-west China. *J. Arid Environ.* **2006**, *64*, 505–522.

19. Xiao, X.; Wang, Y.; Jiang, S.; Ojima, D.S.; Bonham, C.D. Interannual variation in the climate and above-ground biomass of leymus chinense steppe and stipa grandis steppe in the Xilin river basin, inner Mongolia, China. *J. Arid Environ.* **1995**, *31*, 283–299.

20. Bannari, A.; Morin, D.; Bonn, F.; Huete, A. A review of vegetation indices. *Remote Sens. Rev.* **1995**, *13*, 95–120.

21. Jordan, C.F. Derivation of leaf-area index from quality of light on the forest floor. *Ecology* **1969**, *50*, 663–666.

22. Tucker, C.J. Red and photographic infrared linear combinations for monitoring vegetation. *Remote Sens. Environ.* **1979**, *8*, 127–150.

23. Gamon, J.A.; Field, C.B.; Goulden, M.L.; Griffin, K.L.; Hartley, A.E.; Joel, G.; Peñuelas, J.; Valentini, R. Relationships between NDVI, canopy structure, and photosynthesis in three Californian vegetation types. *Ecol. Appl.* **1995**, 28–41.

24. Goetz, S.; Prince, S.D. Modelling terrestrial carbon exchange and storage: Evidence and implications of functional convergence in light-use efficiency. *Adv. Ecol. Res.* **1999**, *28*, 57–92.

25. Myneni, R.B.; Hall, F.G.; Sellers, P.J.; Marshak, A.L. The interpretation of spectral vegetation indexes. *IEEE Trans. Geosci. Remote Sens.* **1995**, *33*, 481–486.

26. Eastman, J.R.; Sangermano, F.; Machado, E.A.; Rogan, J.; Anyamba, A. Global trends in seasonality of normalized difference vegetation index (NDVI), 1982–2011. *Remote Sens.* **2013**, *5*, 4799–4818.

27. Jong, R.; Verbesselt, J.; Schaepman, M.E.; Bruin, S. Trend changes in global greening and browning: Contribution of short-term trends to longer-term change. *Glob.Chang. Biol.* **2012**, *18*, 642–655.

28. Julien, Y.; Sobrino, J. Global land surface phenology trends from GIMMS database. *Int. J. Remote Sens.* **2009**, *30*, 3495–3513.

29. Nemani, R.R.; Keeling, C.D.; Hashimoto, H.; Jolly, W.M.; Piper, S.C.; Tucker, C.J.; Myneni, R.B.; Running, S.W. Climate-driven increases in global terrestrial net primary production from 1982 to 1999. *Science* **2003**, *300*, 1560–1563.

30. Sobrino, J.; Julien, Y. Global trends in NDVI-derived parameters obtained from GIMMS data. *Int. J. Remote Sens.* **2011**, *32*, 4267–4279.

31. Tucker, C.J.; Slayback, D.A.; Pinzon, J.E.; Los, S.O.; Myneni, R.B.; Taylor, M.G. Higher northern latitude normalized difference vegetation index and growing season trends from 1982 to 1999. *Int. J. Biometeorol.* **2001**, *45*, 184–190.

32. Panday, P.K.; Ghimire, B. Time-series analysis of NDVI from AVHRR data over the Hindu Kush-Himalayan region for the period 1982–2006. *Int. J. Remote Sens.* **2012**, *33*, 6710–6721.

33. Kaspersen, P.S.; Fensholt, R.; Huber, S. A spatiotemporal analysis of climatic drivers for observed changes in Sahelian vegetation productivity (1982–2007). *Int. J. Geophys.* **2011**, *2011*, 715321.

34. Fensholt, R.; Rasmussen, K.; Kaspersen, P.; Huber, S.; Horion, S.; Swinnen, E. Assessing land degradation/recovery in the African Sahel from long-term earth observation based primary productivity and precipitation relationships. *Remote Sens.* **2013**, *5*, 664–686.

35. Peng, S.; Chen, A.; Xu, L.; Cao, C.; Fang, J.; Myneni, R.B.; Pinzon, J.E.; Tucker, C.J.; Piao, S. Recent change of vegetation growth trend in China. *Environ. Res. Lett.* **2011**, *6*, 044027.

36. Piao, S.; Fang, J.; Liu, H.; Zhu, B. NDVI-indicated decline in desertification in china in the past two decades. *Geophys. Res. Lett.* **2005**, *32*, doi:10.1029/2004GL021764.

37. Piao, S.; Fang, J.; Zhou, L.; Guo, Q.; Henderson, M.; Ji, W.; Li, Y.; Tao, S. Interannual variations of monthly and seasonal Normalized Difference Vegetation Index (NDVI) in China from 1982 to 1999. *J. Geophys. Res.* **2003**, *108*, doi:10.1029/2002JD002848.

38. Piao, S.; Mohammat, A.; Fang, J.; Cai, Q.; Feng, J. NDVI-based increase in growth of temperate grasslands and its responses to climate changes in China. *Glob. Environ. Chang.* **2006**, *16*, 340–348.

39. Slayback, D.A.; Pinzon, J.E.; Los, S.O.; Tucker, C.J. Northern hemisphere photosynthetic trends 1982–99. *Glob. Chang. Biol.* **2003**, *9*, 1–15.

40. Xu, X.; Piao, S.; Wang, X.; Chen, A.; Ciais, P.; Myneni, R.B. Spatio-temporal patterns of the area experiencing negative vegetation growth anomalies in China over the last three decades. *Environ. Res. Lett.* **2012**, *7*, doi:10.1088/1748-9326/7/3/035701.

41. Peng, J.; Liu, Z.; Liu, Y.; Wu, J.; Han, Y. Trend analysis of vegetation dynamics in Qinghai-Tibet Plateau using Hurst exponent. *Ecol. Indic.* **2012**, *14*, 28–39.

42. Hou, G.; Zhang, H.; Wang, Y. Vegetation dynamics and its relationship with climatic factors in the Changbai mountain natural reserve. *J. Mt. Sci.* **2011**, *8*, 865–875.

43. Coops, N.; Wulder, M.; Duro, D.; Han, T.; Berry, S. The development of a Canadian dynamic habitat index using multi-temporal satellite estimates of canopy light absorbance. *Ecol. Indic.* **2008**, *8*, 754–766.

44. Coops, N.C.; Wulder, M.A.; Iwanicka, D. Demonstration of a satellite-based index to monitor habitat at continental-scales. *Ecol. Indic.* **2009**, *9*, 948–958.

45. Herrmann, S.M.; Anyamba, A.; Tucker, C.J. Recent trends in vegetation dynamics in the African Sahel and their relationship to climate. *Glob. Environ. Chang.* **2005**, *15*, 394–404.

46. Song, Y.; Ma, M. A statistical analysis of the relationship between climatic factors and the Normalized Difference Vegetation Index in China. *Int. J. Remote Sens.* **2011**, *32*, 3947–3965.

47. Nezlin, N.; Kostianoy, A.; Li, B.-L. Inter-annual variability and interaction of remote-sensed vegetation index and atmospheric precipitation in the Aral Sea region. *J. Arid Environ.* **2005**, *62*, 677–700.

48. Wang, J.; Rich, P.; Price, K. Temporal responses of NDVI to precipitation and temperature in the central great plains, USA. *Int. J. Remote Sens.* **2003**, *24*, 2345–2364.

49. Sterling, S.; Ducharne, A. Comprehensive data set of global land cover change for land surface model applications. *Glob. Biogeochem. Cycle* **2008**, *22*, doi:10.1029/2007GB002959.

50. Chen, B.; Xu, G.; Coops, N.C.; Ciais, P.; Innes, J.L.; Wang, G.; Myneni, R.B.; Wang, T.; Krzyzanowski, J.; Li, Q. Changes in vegetation photosynthetic activity trends across the Asia-Pacific region over the last three decades. *Remote Sens. Environ.* **2014**, *144*, 28–41.

51. Holben, B.N. Characteristics of maximum-value composite images from temporal AVHRR data. *Int. J. Remote Sens.* **1986**, *7*, 1417–1434.

52. Liu, S.; Wang, T.; Guo, J.; Qu, J.; An, P. Vegetation change based on SPOT-VGT data from 1998 to 2007, northern China. *Environ. Earth Sci.* **2010**, *60*, 1459–1466.

53. Saha, S.; Moorthi, S.; Wu, X.; Wang, J.; Nadiga, S.; Tripp, P.; Pan, H.-L.; Behringer, D.; Hou, Y.-T.; Chuang, H.-y. The NECP climate forecast system version 2. *J. Clim.* **2012**, *27*, 2185–2208.

54. Saha, S.; Nadiga, S.; Thiaw, C.; Wang, J.; Wang, W.; Zhang, Q.; van den Dool, H.; Pan, H.-L.; Moorthi, S.; Behringer, D. The NCEP climate forecast system. *J. Clim.* **2006**, *19*, 3483–3517.

55. Zhang, X.; Sun, S.; Yong, S.; Zhou, Z.; Wang, R. *Vegetation Map of the People's Republic of China (1: 1000000)*; Geological Publishing House: Beijing, China, 2007.

56. Toms, J.D.; Lesperance, M.L. Piecewise regression: A tool for identifying ecological thresholds. *Ecology* **2003**, *84*, 2034–2041.

57. Francesco Ficetola, G.; Denoël, M. Ecological thresholds: An assessment of methods to identify abrupt changes in species-habitat relationships. *Ecography* **2009**, *32*, 1075–1084.

58. Sun, J.; Wang, X.; Chen, A.; Ma, Y.; Cui, M.; Piao, S. NDVI indicated characteristics of vegetation cover change in China's metropolises over the last three decades. *Environ. Monit. Assess.* **2011**, *179*, 1–14.

59. Swift, T.L.; Hannon, S.J. Critical thresholds associated with habitat loss: A review of the concepts, evidence, and applications. *Biol. Rev.* **2010**, *85*, 35–53.

60. Wang, S.; Wang, Z.; Piao, S.; Fang, J. Regional differences in the timing of recent air warming during the past four decades in China. *Chin. Sci. Bull.* **2010**, *55*, 1968–1973.

61. Akaike, H. A new look at the statistical model identification. *IEEE Trans. Autom. Control* **1974**, *19*, 716–723.

62. Burnham, K.P.; Anderson, D.R. *Model. Selection and Multi-Model Inference: A Practical Information-Theoretic Approach*; Springer: New York, NY, USA, 2002.

63. Ren, J.; Liu, H.; Yin, Y.; He, S. Drivers of greening trend across vertically distributed biomes in temperate arid Asia. *Geophy. Res. Lett.* **2007**, *34*, L07707.

64. Games, P.A.; Howell, J.F. Pairwise multiple comparison procedures with unequal n's and/or variances: A Monte Carlo study. *J. Educ. Behav. Statist.* **1976**, *1*, 113–125.

65. Liu, S.; Gong, P. Change of surface cover greenness in China between 2000 and 2010. *Chin. Sci. Bull.* **2012**, *57*, 2835–2845.

66. Mao, D.; Wang, Z.; Luo, L.; Ren, C. Integrating AVHRR and MODIS data to monitor NDVI changes and their relationships with climatic parameters in northeast China. *Int. J. Appl. Earth Obs. Geoinf.* **2012**, *18*, 528–536.

67. Yan, J.; Chen, B.; Fang, S.; Zhang, H.; Fu, D.; Xue, Y. The response of vegetation index to drought: Taking the extreme drought disaster between 2009 and 2010 in southwest China as an example. *J. Remote Sens.* **2012**, *16*, 720–737.

68. Hintze, J.L.; Nelson, R.D. Violin plots: A box plot-density trace synergism. *Am. Statist.* **1998**, *52*, 181–184.

69. Zhou, H.; Zhao, X.; Tang, Y.; Gu, S.; Zhou, L. Alpine grassland degradation and its control in the source region of the Yangtze and Yellow Rivers, China. *Grassl. Sci.* **2005**, *51*, 191–203.

70. Cui, X.; Graf, H.-F. Recent land cover changes on the Tibetan Plateau: A review. *Clim. Chang.* **2009**, *94*, 47–61.

71. Wang, J.; Price, K.; Rich, P. Spatial patterns of NDVI in response to precipitation and temperature in the central great plains. *Int. J. Remote Sens.* **2001**, *22*, 3827–3844.